ANL-7853

ANL-7853

# ENERGY-DEPENDENT TRANSPORT THEORY WITH A SEPARABLE KERNEL

H. A. Larson

U of C-AUA-USAEC

ARGONNE NATIONAL LABORATORY, ARGONNE, ILLINOIS

The facilities of Argonne National Laboratory are owned by the United States Government. Under the terms of a contract (W-31-109-Eng-38) between the U. S. Atomic Energy Commission, Argonne Universities Association and The University of Chicago, the University employs the staff and operates the Laboratory in accordance with policies and programs formulated, approved and reviewed by the Association.





Printed in the United States of America
Available from
National Technical Information Service
U.S. Department of Commerce
5285 Port Royal Road
Springfield, Virginia 22151
Price: Printed Copy \$3.00; Microfiche \$0.95

ANL-7853
Physics

ARGONNE NATIONAL LABORATORY
9700 South Cass Avenue
Argonne, Illinois 60439

# ENERGY-DEPENDENT TRANSPORT THEORY WITH A SEPARABLE KERNEL

by

H. A. Larson

EBR-II Project

Based in part on a dissertation
submitted to the University of Washington
in partial fulfillment of the
requirements for the degree of
Doctor of Philosophy

October 1971

# TABLE OF CONTENTS

## LIST OF FIGURES



## LIST OF TABLES

ENERGY-DEPENDENT TRANSPORT THEORY
WITH A SEPARABLE KERNEL

by

H. A. Larson

ABSTRACT

The energy- and angle-dependent reflection and transmission distributions for the slab-albedo problem are obtained for scattering described by a separable kernel. These solutions follow by relating the solution of the nonlinear, invariant-imbedding integral equations to the end point values of an inhomogeneous, linear Fredholm integral equation. Use of a stochastic description also permits determination of the mean number of collisions suffered by a particle before it emerges from a face of the slab. Numerical results are obtained for neutrons incident upon a free gas.

## I. INTRODUCTION

Techniques such as the discrete-ordinates,[1] Monte-Carlo,[2] and spherical-harmonics methods[3] can be used to determine the energy-dependent reflection and transmission distribution of particles in the infinite-slab problem. Each of these methods, however, has limitations for the solution of thin-slab problems. Furthermore, the neutron distribution (or photon intensity) must be determined throughout the slab with constraints provided at the region boundaries; if only the emerging distributions are required, the solution in the interior need not be obtained if the invariant-imbedding method is used. Invariant imbedding differs from the other methods in that it concentrates on the particle fluxes crossing the slab boundaries as a function of the changing thickness of the slab; numerically, this method is best suited for thinner slabs. To formulate the nonlinear, integrodifferential equations characteristic of the method, either the approach of Wing[4] or that of Chandrasekhar[5] may be used.

Classical numerical approaches for solution of a system of initial-value differential equations from invariant-imbedding theory have been employed by Mathews _et al_.[6] and Mockel[7] to obtain the reflected and transmitted distributions for energy-dependent problems. A second numerical approach, the transmission-matrix method,[8] can also be used to solve equations of the invariant-imbedding type. This method requires the diagonalization and inversion of the matrix containing the material properties of the slab and the subsequent combination of this information into an overall transfer matrix that contains the reflection and transmission matrices. A third approach was developed by Busbridge,[9] who related the one-speed coupled integral equations of invariant imbedding to the end point values of a linear integral equation.

This report extends the work of Busbridge[9] for the transmission and reflection distributions of a slab in order to do calculations where scattering is described by a separable[10-13] kernel. It will be shown that the distributions may be obtained from the solutions of two nonlinear, coupled integral equations, which are similar to the X- and Y-equations of Chandrasekhar.[5]

In energy-dependent theory, the X- and Y-type equations are obtained only if the scattering kernel is assumed separable, as demonstrated by Sobouti.[14] Solutions of the coupled integral equations can be related to the end point values of a single, inhomogeneous Fredholm integral equation. For computations, it is advantageous to keep the slab thickness small in order that the Neumann series for the Fredholm integral equation converge with a reasonable number of terms. Hence the technique is best suited to thin slabs.

The calculated reflection and transmission functions can also be used to yield information about the mean number of scatterings experienced by a neutron emerging from the slab. The work of Sobolev[15-18] explored this quantity in radiative transfer, including the possibility of a frequency change in the photon during scattering. In one-speed, neutron-transport theory, Abu-Shumays[19] showed that the mean number of collisions and the variance could be simply determined by the use of a "stochastic" value for the mean number of secondaries in the solution of the transport equation. An extension of the Abu-Shumays procedure to energy-dependent theory is presented here. Such information may be useful in the future development of techniques to correct for multiple scattering effects in experimental transmission measurements of cross sections.[20]

The method of solution used here has the advantage that it is not a multigroup method. Quantities of interest are all continuous in energy and angle, subject only to quadrature approximations; hence one need not average physical quantities over an energy interval. A limitation of the procedure used here is that the scattering kernel is somewhat restrictive and tends to be too strong a thermalizer, although many features of neutron-transport phenomena can be derived while using it.[7,10-13]

The scattering properties of real moderators are sometimes too complicated to be rigorously taken into account in transport problems; also, finer details of the scattering function may have little influence upon the solution of the transport equation. For both of these reasons, scattering models are developed that at least roughly approach the real scattering laws while preserving the basic features of the scattering phenomenon. Additionally, models that are purely artificial inventions aid in the development of methods for solving the transport equation.[21]

The usual approach with respect to the angular dependence of the scattering kernel is to make an expansion in Legendre polynomials and truncate the series. New theories are usually developed with only the zeroth, or isotropic, Legendre term retained in the expansion; later developments of these theories may include a refined scattering kernel accounting for (at least) linear anisotropic scattering. Any terms beyond the linear term are usually ignored because they are considered relatively unimportant for neutron-transport calculations at low energies and for nonhydrogeneous materials.

With regard to energy dependence, the simplest artificial kernel is the constant-cross-section approximation, which is equivalent to a one-speed problem.[22] More refined kernels are the Fermi kernel, which describes the scattering by a delta function in energy,[23] and the degenerate kernel, which describes the scattering in terms of a bilinear series.[24] Several kernels that are based on physical principles are available. Perhaps the most widely used of these is the monatomic gas model, which has also been used quite extensively to describe nongaseous moderators.[10] Other available models are based on the structure and dynamics of various moderators.[12]

The Fermi kernel represents one extreme in describing the energy exchange in a scattering, since it represents very weak energy exchange between moderator atoms and neutrons. The separable kernel, consisting only of the first (isotropic) term of the degenerate kernel, represents the other extreme; for this kernel, the medium has very strong thermalizing properties, virtually casting a neutron into equilibrium with the moderator after a single collision.[10]

Perhaps the most rewarding use of the degenerate kernel with a given number of terms occurs when it is expanded in moments of the scattering kernel. Then each successive term accounts exactly for a higher moment of the scattering kernel.[10] (In contrast to this, a polynomial expansion model will represent each moment only as accurately as the truncation will permit.) Furthermore, the degenerate kernel has the desirable property that it satisfies detailed balance. This kernel also preserves the scattering cross section exactly, a desirable trait when leakage fluxes are required. From a mathematical standpoint, another valuable asset of the degenerate kernel is that it greatly facilitates the solution of the transport equation. The degeneracy of the kernel causes a decoupling of the initial neutron energy from the neutron energy after the scattering interaction. It is this type of separable kernel that will be used in this report.

# II. THEORETICAL DEVELOPMENT

## A. Basic Equations

The basic equation describing neutron motion is the transport equation which we shall assume has the simplified form[25]

$$\left[\frac{\mu}{\Sigma_t(\epsilon)}\frac{\partial}{\partial x}+1\right]\Psi(0,\epsilon_0,\mu_0\rightarrow x,\epsilon,\mu)=$$

$$\int_0^\infty d\epsilon'\int_{-1}^{1}d\mu'\,\Sigma(\epsilon',\mu'\rightarrow\epsilon,\mu)\,\frac{\Psi(0,\epsilon_0,\mu_0\rightarrow x,\epsilon',\mu')}{\Sigma_t(\epsilon')},\tag{1}$$

where $\Psi(0,\epsilon_0,\mu_0\rightarrow x,\epsilon,\mu)$ is the collision density at energy $\epsilon$ (normalized to units of kT) and direction $\cos^{-1}\mu$. The total macroscopic cross section of the medium is $\Sigma_t(\epsilon)$. Equation 1 is to be solved subject to the boundary conditions for the slab of thickness $\tau$

$$\Psi(0,\epsilon_0,\mu_0\rightarrow 0,\epsilon,\mu)=\frac{1}{2\pi}\,\delta(\epsilon-\epsilon_0)\,\delta(\mu-\mu_0),\qquad 0\le\mu\le 1;$$

$$\Psi(0,\epsilon_0,\mu_0\rightarrow\tau,\epsilon,-\mu)=0,\qquad 0\le\mu\le 1.$$

The one-term kernel describing the scattering from state $(\epsilon',\mu')$ to state $(\epsilon,\mu)$ is specified by the relation

$$\Sigma(\epsilon',\mu'\rightarrow\epsilon,\mu)=\frac{1}{2}M(\epsilon)\,\frac{\Sigma_s(\epsilon')\Sigma_s(\epsilon)}{\overline{\Sigma}},\tag{2}$$

where $\overline{\Sigma}$ is the angle- and Maxwellian-averaged scattering cross section for $\Sigma_s(\epsilon)$, and $M(\epsilon)$ is the normalized Maxwellian distribution. The form of the kernel is seen to satisfy the detailed balance relation and specifically precludes the fission process.

With this kernel it is possible to cast the four nonlinear, invariant-imbedding, integrodifferential equations into the form of two nonlinear integral equations given by[7]

$$\psi(\tau,\epsilon,\mu)=\Sigma_s(\epsilon)+\frac{1}{2}\int_0^\infty d\epsilon_0\int_0^1\frac{d\mu_0}{\mu_0}\,\frac{M(\epsilon_0)\Sigma_s(\epsilon_0)}{\Sigma_t(\epsilon_0)/\mu_0+\Sigma_t(\epsilon)/\mu}$$

$$\cdot\left[\psi(\tau,\epsilon,\mu)\psi(\tau,\epsilon_0,\mu_0)-\varphi(\tau,\epsilon,\mu)\varphi(\tau,\epsilon_0,\mu_0)\right];\tag{3}$$

$$\varphi(\tau, \epsilon, \mu) = \Sigma_s(\epsilon)e^{-\Sigma_t(\epsilon)/\mu} + \frac{1}{2}\int_0^\infty d\epsilon_0 \int_0^1 \frac{d\mu_0}{\mu_0} \frac{M(\epsilon_0)\Sigma_s(\epsilon_0)}{\Sigma_t(\epsilon_0)/\mu_0 - \Sigma_t(\epsilon)/\mu}$$

$$\cdot [\varphi(\tau, \epsilon, \mu)\psi(\tau, \epsilon_0, \mu_0) - \psi(\tau, \epsilon, \mu)\varphi(\tau, \epsilon_0, \mu_0)]. \quad (4)$$

The functions $\psi(\tau, \epsilon, \mu)$ and $\varphi(\tau, \epsilon, \mu)$ are defined in a manner similar to their description in Ref. 7:

$$\psi(\tau, \epsilon, \mu) = \Sigma_s(\epsilon) + \frac{1}{M(\epsilon)}\int_0^\infty d\epsilon_0 \int_0^1 d\mu_0 R(\tau, \epsilon, \mu; \epsilon_0, \mu_0)\Sigma_s(\epsilon_0)M(\epsilon_0); \quad (5)$$

$$\varphi(\tau, \epsilon, \mu) = \frac{1}{M(\epsilon)}\int_0^\infty d\epsilon_0 \int_0^1 d\mu_0 T(\tau, \epsilon, \mu; \epsilon_0, \mu_0)\Sigma_s(\epsilon_0)M(\epsilon_0). \quad (6)$$

The transmission function $T(\tau, \epsilon, \mu; \epsilon_0, \mu_0)\, d\epsilon\, d\mu$ is defined as the probability that a particle incident upon the slab face at $x = 0$ in a direction whose cosine is $\mu_0$ and with energy $\epsilon_0$ will emerge at the slab face at $x = \tau$ with a direction in $d\mu$ about $\mu$ and an energy in $d\epsilon$ about $\epsilon$. An analogous definition holds for the reflection function given by $R(\tau, \epsilon, \mu; \epsilon_0, \mu_0)\, d\epsilon\, d\mu$.

B. Emergent Collision Densities and Linear Integral Equation

The reflection and transmission functions are very simply related to the collision densities at the slab surfaces by the equations

$$R(\tau, \epsilon, \mu; \epsilon_0, \mu_0) = 2\pi \frac{\mu\Sigma_t(\epsilon)}{\mu_0\Sigma_t(\epsilon_0)} \Psi(0, \epsilon_0, \mu_0 \to 0, \epsilon, -\mu) \quad (7)$$

and

$$T(\tau, \epsilon, \mu; \epsilon_0, \mu_0) = 2\pi \frac{\mu\Sigma_t(\epsilon)}{\mu_0\Sigma_t(\epsilon_0)} \Psi(0, \epsilon_0, \mu_0 \to \tau, \epsilon, \mu), \quad (8)$$

where $0 \le \mu \le 1$. We observe that $\psi(\tau, \epsilon, \mu)$ and $\varphi(\tau, \epsilon, \mu)$ are the energy-dependent counterparts of the X- and Y-functions of Chandrasekhar[5] for the separable kernel. Once these functions have been determined, the reflection and transmission distributions can be obtained from the equations[7]

$$R(\tau, \epsilon, \mu; \epsilon_0, \mu_0) = \frac{M(\epsilon)}{2\mu_0}\left[\frac{\psi(\tau, \epsilon, \mu)\psi(\tau, \epsilon_0, \mu_0) - \varphi(\tau, \epsilon, \mu)\varphi(\tau, \epsilon_0, \mu_0)}{\Sigma_t(\epsilon_0)/\mu_0 + \Sigma_t(\epsilon_0)/\mu}\right] \quad (9)$$

and

$$T(\tau, \epsilon, \mu; \epsilon_0, \mu_0) = \exp[-\Sigma_t(\epsilon_0)/\mu_0]\delta(\epsilon - \epsilon_0)\ \delta(\mu - \mu_0)$$
$$+ \frac{M(\epsilon)}{2\mu_0}\left[\frac{\varphi(\tau, \epsilon, \mu)\psi(\tau, \epsilon_0, \mu_0) - \psi(\tau, \epsilon, \mu)\varphi(\tau, \epsilon_0, \mu_0)}{\Sigma_t(\epsilon_0)/\mu_0 - \Sigma_t(\epsilon)/\mu}\right]. \tag{10}$$

It is seen from Eqs. 9 and 10 that R and T satisfy the reciprocity relations[7]

$$\mu_0 M(\epsilon_0)R(\tau, \epsilon, \mu; \epsilon_0, \mu_0) = \mu M(\epsilon)R(\tau, \epsilon_0, \mu_0; \epsilon, \mu)$$

and

$$\mu_0 M(\epsilon_0)T(\tau, \epsilon, \mu; \epsilon_0, \mu_0) = \mu M(\epsilon)T(\tau, \epsilon_0, \mu_0; \epsilon, \mu),$$

which, through use of Eqs. 7 and 8, agree with the reciprocity relations given in Ref. 25.

Equations 3 and 4 are the coupled integral equations that describe the diffuse reflection and transmission properties of the slab. The equations correctly reduce to the single nonlinear equation describing half-space reflection, since the function $\varphi(\infty, \epsilon, \mu)$ is zero. Furthermore, it can be shown[25] that the reduced equation in terms of $\psi(\infty, \epsilon, \mu)$ can be cast into the form of the equation for the H-function of Chandrasekhar.[5]

Equations 3 and 4 are solved by considering the linear Fredholm equation

$$(I - L)_x \{J(t, \epsilon, \mu)\} = \exp[-\Sigma_t(\epsilon)x/\mu], \tag{11}$$

where the operator $L_x\{J(t,\epsilon,\mu)\}$ is defined as

$$L_x\{J(t, \epsilon, \mu)\} = \int_0^\tau K_1(|t - x|)\ J(t, \epsilon, \mu)\ dt, \tag{12}$$

and where the kernel $K_1$ is defined by

$$K_n(\eta) = \frac{1}{2\Sigma}\int_0^\infty d\epsilon \int_0^1 \frac{d\mu}{\mu}\ M(\epsilon)\left[\frac{\mu}{\Sigma_t(\epsilon)}\right]^{n-1} \Sigma_s^2(\epsilon)\ \exp[-\Sigma_t(\epsilon)\eta/\mu], \tag{13}$$

$$n = 1, 2, \ldots .$$

(The need for $K_n(\eta)$, $n > 1$, occurs in the numerical evaluation scheme of Sec. D below.) Equations 11 and 12 are the energy-dependent generalizations of the "auxiliary equation" of Busbridge,[9] and $J(t, \epsilon, \mu)$ is the energy-dependent "auxiliary function." It will be shown below that $J(0, \epsilon, \mu)$ and $J(\tau, \epsilon, \mu)$ may be related directly to $\psi(\tau, \epsilon, \mu)$ and $\varphi(\tau, \epsilon, \mu)$, respectively.

To establish the connection between Eqs. 3 and 4 and the auxiliary equation, two lemmas are used.

Lemma 1. Let

$$F_1(x, \epsilon, \mu) = \frac{J(0, \epsilon, \mu)}{2\overline{\overline{\Sigma}}} \int_0^\infty d\epsilon_0 \int_0^1 \frac{d\mu_0}{\mu_0} M(\epsilon_0)\Sigma_s^2(\epsilon_0)J(x, \epsilon_0, \mu_0)$$

$$- \frac{J(\tau, \epsilon, \mu)}{2\overline{\overline{\Sigma}}} \int_0^\infty d\epsilon_0 \int_0^1 \frac{d\mu_0}{\mu_0} M(\epsilon_0)\Sigma_s^2(\epsilon_0)J(\tau - x, \epsilon_0, \mu_0).$$

Then

$$(I - L)_x \{F_1(t, \epsilon, \mu)\} = J(0, \epsilon, \mu)K_1(x) - J(\tau, \epsilon, \mu)K_1(\tau - x).$$

Proof: This lemma is proved, in part, by using Eqs. 11 and 12 in Eq. 13 to observe that

$$K_1(x) = \frac{1}{2\overline{\overline{\Sigma}}} \int_0^\infty d\epsilon_0 \int_0^1 \frac{d\mu_0}{\mu_0} M(\epsilon_0)\Sigma_s^2(\epsilon_0)J(x, \epsilon_0, \mu_0)$$

$$- \frac{1}{2\overline{\overline{\Sigma}}} \int_0^\infty d\epsilon_0 \int_0^1 \frac{d\mu_0}{\mu_0} M(\epsilon_0)\Sigma_s^2(\epsilon_0) \int_0^\tau K_1(|t - x|)\, J(t, \epsilon_0, \mu_0)\, dt$$

$$= (I - L)_x \left\{ \frac{1}{2\overline{\overline{\Sigma}}} \int_0^\infty d\epsilon_0 \int_0^1 \frac{d\mu_0}{\mu_0} M(\epsilon_0)\Sigma_s^2(\epsilon_0)J(t, \epsilon_0, \mu_0) \right\},$$

where the last step is accomplished by an interchange of the order of integration. The proof is completed by writing this last equation for $K_1(x)$ and $K_1(\tau - x)$, multiplying by $J(0, \epsilon, \mu)$ and $J(\tau, \epsilon, \mu)$, respectively, and then subtracting.

Lemma 2. Let

$$F_2(x, \epsilon, \mu) = \frac{\partial J(x, \epsilon, \mu)}{\partial x} + \frac{\Sigma_t(\epsilon)}{\mu} J(x, \epsilon, \mu).$$

Then

$$(I - L)_x \{F_2(t, \epsilon, \mu)\} = J(0, \epsilon, \mu)K_1(x) - J(\tau, \epsilon, \mu)K_1(\tau - x).$$

Proof: The proof is given in Appendix A.

The following theorem may now be established:

Theorem

Let $J(0, \epsilon, \mu)$ and $J(\tau, \epsilon, \mu)$ be solutions of the linear Fredholm equation (Eq. 11). Then a solution of the nonlinear, coupled integral Eqs. 3 and 4 is given by

$$\psi(\tau, \epsilon, \mu) = \Sigma_s(\epsilon)J(0, \epsilon, \mu) \tag{14}$$

and

$$\varphi(\tau, \epsilon, \mu) = \Sigma_s(\epsilon)J(\tau, \epsilon, \mu). \tag{15}$$

Proof: Lemmas 1 and 2 give

$$(I - L)_x \{F_1(t, \epsilon, \mu) - F_2(t, \epsilon, \mu)\} = 0,$$

since $L_x$ is a linear operator. As in Ref. 9, it may be shown that the function in braces is zero and hence

$$\frac{\partial J(x, \epsilon, \mu)}{\partial x} + \frac{\Sigma_t(\epsilon)}{\mu} J(x, \epsilon, \mu) = \frac{J(0, \epsilon, \mu)}{2\bar{\Sigma}} \int_0^\infty d\epsilon_0 \int_0^1 \frac{d\mu_0}{\mu_0} M(\epsilon_0)\Sigma_s^2(\epsilon_0)J(x, \epsilon_0, \mu_0)$$

$$- \frac{J(\tau, \epsilon, \mu)}{2\bar{\Sigma}} \int_0^\infty d\epsilon_0 \int_0^1 \frac{d\mu_0}{\mu_0} M(\epsilon_0)\Sigma_s^2(\epsilon_0)J(\tau - x, \epsilon_0, \mu_0). \tag{16}$$

It is now convenient to apply the transform

$$\zeta(s, \epsilon, \mu) = \int_0^\tau e^{-sx}J(x, \epsilon, \mu)\, dx$$

to Eq. 16. Since it follows from Appendix B that

$$\zeta\left[\frac{\Sigma_t(\epsilon_0)}{\mu_0}, \epsilon, \mu\right] = \zeta\left[\frac{\Sigma_t(\epsilon)}{\mu}, \epsilon_0, \mu_0\right] \tag{17}$$

and

$$\exp[-\Sigma_t(\epsilon_0)\tau/\mu_0]\,\zeta\left[-\frac{\Sigma_t(\epsilon_0)}{\mu_0}, \epsilon, \mu\right] = \exp[-\Sigma_t(\epsilon)\tau/\mu]\,\zeta\left[-\frac{\Sigma_t(\epsilon)}{\mu}, \epsilon_0, \mu_0\right], \tag{18}$$

it can then be shown that

$$\left[\frac{\Sigma_t(\epsilon_0)}{\mu_0} + \frac{\Sigma_t(\epsilon)}{\mu}\right]\zeta\left[\frac{\Sigma_t(\epsilon_0)}{\mu_0}, \epsilon, \mu\right] = J(0, \epsilon, \mu)J(0, \epsilon_0, \mu_0) - J(\tau, \epsilon, \mu)J(\tau, \epsilon_0, \mu_0)$$

and

$$\left[\frac{\Sigma_t(\epsilon_0)}{\mu_0} - \frac{\Sigma_t(\epsilon)}{\mu}\right]\zeta\left[-\frac{\Sigma_t(\epsilon_0)}{\mu_0}, \epsilon, \mu\right] = J(0, \epsilon, \mu)J(0, \epsilon_0, -\mu_0) - J(\tau, \epsilon, \mu)J(\tau, \epsilon_0, -\mu_0).$$

At this point, the last two equations are multiplied by $(2\overline{\Sigma}\mu)^{-1}M(\epsilon)\Sigma_s(\epsilon)$ and integrated over $\epsilon$ and $\mu$. The proof of the theorem is then completed with the observation that

$$J(0, \epsilon, -\mu) = \exp[\Sigma_t(\epsilon)\tau/\mu]J(\tau, \epsilon, \mu), \tag{19}$$

a result which is derived in Appendix B.

Solution of Eq. 11 provides a unique answer which, through Eqs. 14, 15, 9, and 10, provides unique transmission and reflection functions whose accuracy depends only upon the accuracy with which Eq. 11 is solved. Direct numerical solution of Eqs. 3 and 4, however, does not necessarily provide a unique solution for $\psi(\tau, \epsilon, \mu)$ and $\varphi(\tau, \epsilon, \mu)$. The uniqueness of the solutions is discussed by Busbridge[9] for the one-speed case and is treated quite extensively by Mullikin.[26] It is sufficient to say here, however, that there are constraint equations[27] that could be applied to the solutions for $\psi(\tau, \epsilon, \mu)$ and $\varphi(\tau, \epsilon, \mu)$. These constraints may be given a physical interpretation, which leads to their immediate derivation.[27,28]

## C. Generating Functions and the Reflection and Transmission Functions

As indicated previously, it is also of interest to obtain information on the mean number of collisions suffered by an incident neutron before it is reflected or transmitted through the slab. Following the approach of Abu-Shumays,[19] the nth-generation transmission, $T_n(\tau, \epsilon, \mu; \epsilon_0, \mu_0)\, d\epsilon\, d\mu$, is defined as the conditional probability that a particle incident upon the slab face at $x = 0$ in a direction whose cosine is $\mu_0$ and with energy $\epsilon_0$ will, after exactly $n$ collisions, emerge from the slab face at $x = \tau$ in a direction whose cosine is in $d\mu$ about $\mu$ and whose energy is in $d\epsilon$ about $\epsilon$. There is a corresponding definition for the nth-generation reflection, $R_n(\tau, \epsilon, \mu; \epsilon_0, \mu_0)\, d\epsilon\, d\mu$. For $\xi \epsilon [0, 1]$, we define density-generating functions by

$$R(\tau, \epsilon, \mu; \epsilon_0, \mu_0; \xi) = \sum_{n=0}^{\infty} \xi^n R_n(\tau, \epsilon, \mu; \epsilon_0, \mu_0) \tag{20}$$

and

$$T(\tau, \epsilon, \mu; \epsilon_0, \mu_0; \xi) = \sum_{n=0}^{\infty} \xi^n T_n(\tau, \epsilon, \mu; \epsilon_0, \mu_0), \tag{21}$$

so that the reflected and transmitted density functions of Eqs. 9 and 10 become

$$R(\tau, \epsilon, \mu; \epsilon_0, \mu_0) = R(\tau, \epsilon, \mu; \epsilon_0, \mu_0; 1) \tag{22}$$

and

$$T(\tau, \epsilon, \mu; \epsilon_0, \mu_0) = T(\tau, \epsilon, \mu; \epsilon_0, \mu_0; 1). \tag{23}$$

In precisely the same manner as in Ref. 19, the invariant-imbedding equations can be manipulated to show that the reflected and transmitted density functions are transformed into the corresponding density-generating functions by replacing the scattering kernel by a "stochastic scattering kernel." For the separable kernel, this stochastic scattering kernel consists of the replacement of $\Sigma_s(\epsilon)$ in Eq. 2 by $\sqrt{\xi}\Sigma_s(\epsilon)$. The invariant-imbedding integral equations for the functions $\psi(\tau, \epsilon, \mu; \xi)$ and $\varphi(\tau, \epsilon, \mu; \xi)$ can then be written in a form similar to Eqs. 3 and 4 after replacement of $\Sigma_s(\epsilon)$ by $\sqrt{\xi}\Sigma_s(\epsilon)$. In this case, the generating functions $R(\tau, \epsilon, \mu; \epsilon_0, \mu_0; \xi)$ and $T(\tau, \epsilon, \mu; \epsilon_0, \mu_0, \xi)$ obey Eqs. 9 and 10, with $\psi(\tau, \epsilon, \mu)$ and $\varphi(\tau, \epsilon, \mu)$ replaced by $\psi(\tau, \epsilon, \mu; \xi)$ and $\varphi(\tau, \epsilon, \mu; \xi)$, respectively. The functions $\psi(\tau, \epsilon, \mu; \xi)$ and $\varphi(\tau, \epsilon, \mu; \xi)$ satisfy equations similar to Eqs. 14 and 15:

$$\psi(\tau, \epsilon, \mu; \xi) = \sqrt{\xi}\Sigma_s(\epsilon)J(0, \epsilon, \mu; \xi) \tag{24}$$

and

$$\varphi(\tau, \epsilon, \mu; \xi) = \sqrt{\xi}\Sigma_s(\epsilon)J(\tau, \epsilon, \mu; \xi). \tag{25}$$

Here $J(\tau, \epsilon, \mu; \xi)$ satisfies auxiliary Eq. 11 with a kernel $K_1(\eta; \xi)$ of Eq. 12, now defined by

$$K_1(\eta; \xi) = \xi K_1(\eta), \tag{26}$$

where $K_1(\eta)$ is defined in Eq. 13. Thus, all stochastic dependence resides as a multiplier of the kernel.

From Eqs. 20 and 21, we observe that the mean number of collisions, $\bar{n}_r$ and $\bar{n}_t$, for the reflection and transmission of neutrons, respectively, can be determined from the equations

$$\bar{n}_r = \frac{\sum_{m=0}^{\infty} m R_m(\tau, \epsilon, \mu; \epsilon_0, \mu_0)}{\sum_{m=0}^{\infty} R_m(\tau, \epsilon, \mu; \epsilon_0, \mu_0)} = \frac{\frac{\partial}{\partial \xi} R(\tau, \epsilon, \mu; \epsilon_0, \mu_0; \xi)\Big|_{\xi=1}}{R(\tau, \epsilon, \mu; \epsilon_0, \mu_0; 1)} \tag{27}$$

and

$$\bar{n}_t = \frac{\sum_{m=0}^{\infty} m T_m(\tau, \epsilon, \mu; \epsilon_0, \mu_0)}{\sum_{m=0}^{\infty} T_m(\tau, \epsilon, \mu; \epsilon_0, \mu_0)} = \frac{\frac{\partial}{\partial \xi} T(\tau, \epsilon, \mu; \epsilon_0, \mu_0; \xi)\Big|_{\xi=1}}{T(\tau, \epsilon, \mu; \epsilon_0, \mu_0; 1)} . \tag{28}$$

Further, the variance in each of the quantities can be determined from

$$\overline{n_r(n_r - 1)} = \frac{\frac{\partial^2}{\partial \xi^2} R(\tau, \epsilon, \mu; \epsilon_0, \mu_0; \xi)\Big|_{\xi=1}}{R(\tau, \epsilon, \mu; \epsilon_0, \mu_0; 1)} \tag{29}$$

and

$$\overline{n_t(n_t - 1)} = \frac{\frac{\partial^2}{\partial \xi^2} T(\tau, \epsilon, \mu; \epsilon_0, \mu_0; \xi)\Big|_{\xi=1}}{T(\tau, \epsilon, \mu; \epsilon_0, \mu_0; 1)} \tag{30}$$

through the relations

$$\mathrm{Var}(\bar{n}_r) = \overline{n_r(n_r - 1)} + \bar{n}_r - \bar{n}_r^2 \tag{31}$$

and

$$\mathrm{Var}(\bar{n}_t) = \overline{n_t(n_t - 1)} + \bar{n}_t - \bar{n}_t^2 . \tag{32}$$

## D. Calculational Procedure

Numerical solution of Eq. 11 and subsequent use of Eqs. 14 and 15, 9 and 10, and 7 and 8 yield the energy- and angle-dependent reflected and transmitted distributions for a unit neutron source impinging upon a face of the slab. This numerical solution is by no means trivial, because there is a logarithmic singularity in the kernel $K_1(\eta)$ of Eq. 13 when $\eta$ is near zero. This numerical procedure could be avoided by use of the technique employed by Mockel (Eqs. 34 and 40 of Ref. 7) who obtained the functions $\psi(\tau, \epsilon, \mu)$ and $\varphi(\tau, \epsilon, \mu)$ by a direct (initial-value) numerical solution of a coupled pair of nonlinear, first-order integrodifferential equations. The solution of Eq. 11, however, allows the determination of the reflection and transmission functions at specified angles and energies, instead of angles and energies restricted to a mesh chosen strictly for best numerical evaluation of the integrals.

One way to numerically solve Eq. 11 is to expand the function $J(\tau, \epsilon, \mu)$ in a truncated power series given by

$$J(\tau, \epsilon, \mu) = \sum_{n=0}^{N} a_n(\epsilon, \mu) t^n. \tag{33}$$

Equation 33 allows us to write Eq. 12 as

$$L_x\{J(t, \epsilon, \mu)\} = \sum_{n=0}^{N} a_n(\epsilon, \mu) I_n(x, \tau), \tag{34}$$

where

$$I_n(x, \tau) = \int_0^{\tau} K_1(|t - x|)\, t^n\, dt.$$

We recognize that $I_n(x, \tau)$ can now be explicitly determined by parts integrations since, from Eq. 13,

$$K_n(\eta) = (-1)^n \frac{d}{d\eta} K_{n+1}(\eta).$$

At this point we note that the straightforward substitution of Eq. 33 into Eq. 11 will define a set of $N + 1$ equations in the coefficients $a_n(\epsilon, \mu)$, whose order depends upon the order of the polynomial expansion in Eq. 33. Determination of the $a_n(\epsilon, \mu)$ leads directly to $J(\tau, \epsilon, \mu)$. As the size of the slab increases, however, one is forced to increase $N$ to obtain the desired accuracy.

A means of avoiding the higher-order polynomials can be obtained by generalizing the approach of Mayers.[29] This consists of dividing the slab into $K$ subslabs of half-width $t_k$ and treating each subslab with a low $N$th-order polynomial fit. We assume a set of $N + 1$ mesh points for each subslab and, since $I_n(x, \tau)$ is known, a change of variable allows the explicit determination of $b_{ki}(x, \tau)$ from a quadrature formula given by

$$I_{kn}(x, \tau) = \int_{-t_k}^{t_k} K_1(|y - x|)\, y^n\, dy = \sum_{i=0}^{N} b_{ik}(x, \tau) y_{ik}^n, \quad k = 1, 2, \ldots, K. \tag{35}$$

We now substitute Eq. 35 into Eq. 11 to give

$$J(x, \epsilon, \mu) = \sum_{k=1}^{K} \sum_{n=0}^{N} a_{nk}(\epsilon, \mu) \sum_{i=0}^{N} b_{ik}(x, \tau) y_{ik}^{n} + \exp[-\Sigma_t(\epsilon)x/\mu]$$

and rearrange to obtain

$$J(x, \epsilon, \mu) = \sum_{k=1}^{K} \sum_{i=0}^{N} b_{ik}(x, \tau) J(y_{ik}, \epsilon, \mu) + \exp[-\Sigma_t(\epsilon)x/\mu], \qquad (36)$$

where

$$J(y_{ik}, \epsilon, \mu) = \sum_{n=0}^{N} a_{nk}(\epsilon, \mu) y_{ik}^{n}, \quad i = 0, 1, \ldots, N, \ k = 1, 2, \ldots, K.$$

Evaluation of Eq. 36 at each of the prescribed $K(N+1)$ points of the slab and provision of coupling between the subslabs by setting $J(y_{Nk}, \epsilon, \mu) = J(y_{0k+1}, \epsilon, \mu)$ enables us to find a vector $J(\tau, \epsilon, \mu)$ across the slab $(0, \tau)$.

The approach of Mayers was chosen because the straightforward substitution of Eq. 33 into Eq. 11 led to the inversion of an ill-conditioned matrix and also showed no significant decrease in computer running time when compared with the method of Eq. 36. We also note that the angle and energy dependence in Eq. 36 reside entirely in the exponential, so that to calculate $J(\tau, \epsilon, \mu)$ for various values of $\epsilon$ and $\mu$, we merely reiterate the equation with the matrix composed of the $b_{ki}(x, \tau)$ for the slab.

Numerical differentiations as indicated by Eqs. 27-30 were performed to determine the mean number of collisions and the variance. Since the order of the error in the derivative when using a two-point differencing scheme is of the order of the mesh spacing, and since this was assumed to be 0.01 in the calculations, a two-point difference for the first derivative and a three-point difference for the second derivative were used. Thus, when variance calculations were desired, three solutions of the integral equation were made. An extension of the calculational procedure to higher-point difference approximations would not be infeasible, however, since each solution of the integral equation required approximately 0.55 sec on a CDC-6400 computer.

## III. NUMERICAL RESULTS

A computer code was written to solve Eq. 11 and to evaluate Eqs. 27-30. The accuracy of the code was confirmed by the reproduction of the one-speed data given by Bellman et al.[30] and by the solution of an equation with an analytic answer. Numerical results for the energy-dependent theory were obtained using the scattering cross section $\Sigma_s(\epsilon)$ given[12] by the zeroth moment of the scattering kernel for a free gas,

$$\Sigma_s(\epsilon) = \frac{\Sigma_f}{2A\epsilon}\left[(2A\epsilon+1)\,\mathrm{erf}\,(\sqrt{A\epsilon}) + 2\sqrt{A\epsilon/\pi}\,e^{-A\epsilon}\right], \tag{37}$$

where A is the ratio of scatterer to neutron mass and $\Sigma_f$ is the free atom cross section. The constant $\bar{\Sigma}$ in Eq. 2 is given by

$$\bar{\Sigma} = \Sigma_f\left(1 + \frac{1}{A}\right)^{1/2},$$

where the values of $\Sigma_f$ are given in Table I.

TABLE I. Average Energy and Energy at Maximum of Distribution for Neutrons Reflected and Transmitted in a Nonabsorbing Free Gas, Varying Mass Number A ($\epsilon_0 = 1.0$, $\mu = 1.0$, $\mu_0 = 1.0$, $\tau\Sigma_f = 1/3$)

| | | Reflection | | Transmission | |
|---|---|---|---|---|---|
| A | $\Sigma_f$, cm$^{-1}$ | $\bar{\epsilon}_r$ | $\epsilon_r^*$ | $\bar{\epsilon}_t$ | $\epsilon_t^*$ |
| 1 | 0.00163 | 1.827 ± 0.007 | 0.736 ± 0.004 | 1.830 ± 0.006 | 0.745 ± 0.004 |
| 4 | $1.88 \times 10^{-5}$ | 1.967 ± 0.026 | 0.874 ± 0.016 | 1.967 ± 0.025 | 0.877 ± 0.015 |
| 7 | 0.06280 | 1.986 ± 0.020 | 0.922 ± 0.013 | 1.987 ± 0.020 | 0.924 ± 0.013 |
| 12 | 0.3699 | 1.994 ± 0.014 | 0.953 ± 0.009 | 1.994 ± 0.014 | 0.953 ± 0.009 |
| 18 | 3.4031 | 1.996 ± 0.011 | 0.968 ± 0.007 | 1.996 ± 0.011 | 0.968 ± 0.007 |

The calculations were performed for thin slabs, the observed quantities being the average energy and the most probable energy for neutrons that were reflected and transmitted through the slabs at various angles. To find the average exit energy, it was observed that the data would be fitted very well by a least-squares fit of the exit-energy profiles to the three-parameter functions given by

$$R(\tau, \epsilon, \mu; \epsilon_0, \mu_0) = C_r \epsilon^{\epsilon_r^*/(\bar{\epsilon}_r - \epsilon_r^*)} \exp\left(\frac{-\epsilon}{\bar{\epsilon}_r - \epsilon_r^*}\right) \tag{38}$$

and

$$T(\tau, \epsilon, \mu; \epsilon_0, \mu_0) = C_t \epsilon^{\epsilon_t^*/(\bar{\epsilon}_t - \epsilon_t^*)} \exp\left(\frac{-\epsilon}{\bar{\epsilon}_t - \epsilon_t^*}\right) + \exp[-\Sigma_t(\epsilon_0)\tau/\mu_0]\,\delta(\epsilon - \epsilon_0)\,\delta(\mu - \mu_0). \tag{39}$$

Here $\bar{\epsilon}$ and $\epsilon^*$ are constants denoting the average neutron energy and the energy at the maximum of the distribution, respectively; these constants take on the values $\bar{\epsilon} = 2$ and $\epsilon^* = 1$ for a purely Maxwellian distribution. $C_r$ and $C_t$ are fitting parameters.

Table I shows sample values of least-squares-fitted coefficients of $\bar{\varepsilon}$ and $\varepsilon^*$ for a conservative system. The heavier target materials produce emergent distributions that are not far from the Maxwellian in shape. As A decreases, the departure from Maxwellian is quite evident, but the shape is very easily fitted to functions of the form of Eqs. 38 and 39. The error range quoted in Table I is a consequence of the use of a nonlinear least-squares-fitting routine.

Calculations were also made of $\bar{\varepsilon}$ and $\varepsilon^*$ for reflected and transmitted neutrons emergent from nonabsorbing mass-18 gas slabs of varying thickness. The results are shown in Table II, where it was observed that for a given mass number, the average energy of the emergent neutrons approaches the average target energy with increasing slab thickness. This is reasonable, since an increasing slab thickness implies a larger number of collisions, on the average, and hence neutrons escaping from a surface should be nearer equilibrium with the target atoms.

TABLE II. Average Energy and Energy at Maximum of Distribution for Neutrons Reflected and Transmitted in a Nonabsorbing Free Gas, Varying Slab Thickness ($A = 18$, $\varepsilon_0 = 1.0$, $\mu = 1.0$, $\mu_0 = 1.0$)

| | Reflection | | Transmission | |
|---|---|---|---|---|
| $\tau\Sigma_f$ | $\bar{\varepsilon}_r$ | $\varepsilon_r^*$ | $\bar{\varepsilon}_t$ | $\varepsilon_t^*$ |
| 1/6 | 1.996 | 0.965 | 1.996 | 0.965 |
| 1/3 | 1.996 | 0.968 | 1.996 | 0.968 |
| 2/3 | 1.997 | 0.973 | 1.997 | 0.975 |
| 1 | 1.997 | 0.977 | 1.997 | 0.981 |
| 2 | 1.998 | 0.986 | 1.999 | 0.996 |
| 5 | 1.999 | 0.996 | 2.002 | 1.016 |

Figure 1 illustrates the mean number of collisions experienced by a neutron during its migration in a nonabsorbing slab of mass-18 gas of varying thickness. The value of $\bar{n}_r$ for reflected neutrons increases

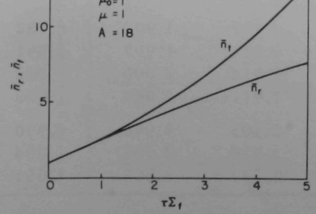


Fig. 1

Mean Number of Collisions Experienced by Reflected and Transmitted Neutrons. ANL Neg. No. 103-A9047.

monotonically and approaches infinity as the slab thickness becomes infinite; a similar result has been explicitly derived for one-speed problems.[19] The value of $\bar{n}_t$ is seen to increase more rapidly than $\bar{n}_r$ for small $\tau$, and likewise increases without bound as the slab thickness increases.

Tables III and IV show the variation with angle of $\bar{\epsilon}$ and $\epsilon^*$ for neutrons reflected and transmitted through conservatively scattering slabs of thickness $\tau\Sigma_f = 1/3$ and 1, respectively, for a scatterer of A = 18. The values of $\bar{\epsilon}$ and $\epsilon^*$ show little dependence upon $\tau$ for $\tau\Sigma_f > 1/3$, but the mean number of collisions before emergence varies substantially. For a given angle of incidence, the average energy of neutrons reflected or transmitted through the slab increases with decreasing $\mu$. In particular, the emergent distribution for the grazing angle appears to be nearly Maxwellian

TABLE III. Average Energy and Energy at Maximum of Distribution for Neutrons Reflected and Transmitted in a Nonabsorbing Free-gas Slab of $\tau\Sigma_f = 1/3$, and Average Number of Collisions Suffered in Transit; A = 18, $\epsilon_0 = 1$

| $\mu_0$ | $\mu$ | $\bar{\epsilon}_r$ | $\epsilon_r^*$ | $\bar{n}_r$ | $\mathrm{Var}(\bar{n}_r)$ | $\bar{\epsilon}_t$ | $\epsilon_t^*$ | $\bar{n}_t$ | $\mathrm{Var}(\bar{n}_t)$ |
|---|---|---|---|---|---|---|---|---|---|
| 1.0 | 1.0 | 1.996 | 0.968 | 1.537 | 0.900 | 1.996 | 0.968 | 1.543 | 0.909 |
| 1.0 | 0.5 | 1.997 | 0.973 | 1.534 | 0.895 | 1.997 | 0.974 | 1.546 | 0.912 |
| 1.0 | 0.02546 | 1.999 | 1.000 | 1.467 | 0.799 | 2.000 | 1.001 | 1.547 | 0.918 |
| 1.0 | 0.005 | 2.000 | 1.000 | 1.463 | 0.791 | 2.000 | 1.000 | 1.547 | 0.916 |
| 0.5 | 1.0 | 1.996 | 0.967 | 1.534 | 0.895 | 1.996 | 0.969 | 1.546 | 0.912 |
| 0.5 | 0.5 | 1.997 | 0.973 | 1.529 | 0.887 | 1.997 | 0.975 | 1.551 | 0.921 |
| 0.5 | 0.02546 | 2.000 | 0.999 | 1.434 | 0.746 | 2.000 | 1.001 | 1.595 | 0.983 |
| 0.5 | 0.005 | 2.000 | 1.000 | 1.428 | 0.735 | 2.000 | 1.000 | 1.596 | 0.982 |
| 0.02546 | 1.0 | 1.996 | 0.964 | 1.467 | 0.799 | 1.997 | 0.973 | 1.547 | 0.917 |
| 0.02546 | 0.5 | 1.996 | 0.966 | 1.434 | 0.747 | 1.997 | 0.983 | 1.594 | 0.981 |
| 0.02546 | 0.02546 | 1.998 | 0.982 | 1.166 | 0.272 | 2.003 | 1.027 | 2.647 | 1.338 |

TABLE IV. Average Energy and Energy at Maximum of Distribution for Neutrons Reflected and Transmitted in a Nonabsorbing Free-gas Slab of $\tau\Sigma_f = 1$, and Average Number of Collisions Suffered in Transit; A = 18, $\epsilon_0 = 1$

| $\mu_0$ | $\mu$ | $\bar{\epsilon}_r$ | $\epsilon_r^*$ | $\bar{n}_r$ | $\bar{\epsilon}_t$ | $\epsilon_t^*$ | $\bar{n}_t$ |
|---|---|---|---|---|---|---|---|
| 1.0 | 1.0 | 1.997 | 0.977 | 2.469 | 1.997 | 0.981 | 2.586 |
| 1.0 | 0.5 | 1.998 | 0.987 | 2.414 | 1.998 | 0.993 | 2.602 |
| 1.0 | 0.02546 | 2.000 | 0.999 | 2.101 | 2.000 | 1.001 | 2.670 |
| 1.0 | 0.005 | 2.000 | 1.000 | 2.099 | 2.000 | 1.000 | 2.669 |
| 0.5 | 1.0 | 1.997 | 0.975 | 2.417 | 1.997 | 0.982 | 2.605 |
| 0.5 | 0.5 | 1.998 | 0.984 | 2.329 | 1.997 | 0.991 | 2.641 |
| 0.5 | 0.02546 | 2.000 | 0.999 | 1.914 | 2.000 | 1.002 | 3.034 |
| 0.5 | 0.005 | 2.000 | 1.000 | 1.911 | 2.000 | 1.000 | 3.034 |
| 0.02546 | 1.0 | 1.996 | 0.968 | 2.103 | 1.998 | 0.990 | 2.665 |
| 0.02546 | 0.5 | 1.997 | 0.970 | 1.914 | 2.000 | 1.008 | 3.019 |
| 0.02546 | 0.02546 | 1.998 | 0.982 | 1.273 | 2.008 | 1.053 | 4.105 |

in shape. This correlates well with the result[10] that the neutron-energy spectrum for neutrons emergent at the grazing angle is Maxwellian for the Milne problem with a degenerate kernel. It would appear that the same is approximately true for the slab-albedo problem, even if the slab is quite thin. Although these conclusions have been reached for an initial energy $\epsilon_0$ near unity, they are expected to be approximately valid for any $\epsilon_0$ because the separable kernel represents a medium with very strong thermalizing properties.[10]

Table V is similar to Table III, except that the data are for a scatterer of A = 1. The average number of collisions required to traverse the slab increases slightly when compared with the A = 18 case of Table III; however, $\bar{\epsilon}$ and $\epsilon^*$ do not indicate emerging spectra as nearly Maxwellian as the A = 18 case except at grazing angles. Figure 2 clearly shows the approach to Maxwellian as the exit angle approaches the grazing angle for a scatterer with A = 1. The leakage spectrum is sub-Maxwellian, a result consistent with the energy of the incident beam, $\epsilon_0 = 1$. To examine the emerging spectrum as a function of energy, the reflection function was calculated using the $\psi(\tau, \epsilon, \mu)$ and $\varphi(\tau, \epsilon, \mu)$ functions, sample values of which are given in Table VI.

TABLE V. Average Energy and Energy at Maximum of Distribution for Neutrons Reflected and Transmitted in a Nonabsorbing Free-gas Slab of $\tau\Sigma_f = 1/3$, and Average Number of Collisions Suffered in Transit; A = 1, $\epsilon_0 = 1$

| $\mu_0$ | $\mu$ | $\bar{\epsilon}_r$ | $\epsilon_r^*$ | $\bar{n}_r$ | Var($\bar{n}_r$) | $\bar{\epsilon}_t$ | $\epsilon_t^*$ | $\bar{n}_t$ | Var($\bar{n}_t$) |
|---|---|---|---|---|---|---|---|---|---|
| 1.0 | 1.0 | 1.827 | 0.736 | 1.629 | 1.122 | 1.830 | 0.745 | 1.637 | 1.135 |
| 1.0 | 0.5 | 1.851 | 0.799 | 1.625 | 1.115 | 1.857 | 0.814 | 1.640 | 1.138 |
| 1.0 | 0.02546 | 1.997 | 0.995 | 1.540 | 0.988 | 2.007 | 1.008 | 1.646 | 1.155 |
| 0.5 | 1.0 | 1.826 | 0.732 | 1.625 | 1.085 | 1.831 | 0.749 | 1.640 | 1.087 |
| 0.5 | 0.5 | 1.849 | 0.792 | 1.617 | 1.076 | 1.859 | 0.821 | 1.648 | 0.999 |
| 0.5 | 0.02546 | 1.992 | 0.989 | 1.496 | 0.893 | 2.013 | 1.014 | 1.711 | 1.238 |
| 0.02546 | 1.0 | 1.811 | 0.683 | 1.544 | 0.995 | 1.846 | 0.798 | 1.646 | 1.139 |
| 0.02546 | 0.5 | 1.841 | 0.741 | 1.506 | 0.930 | 1.867 | 0.871 | 1.690 | 1.217 |
| 0.02546 | 0.02546 | 1.895 | 0.856 | 1.194 | 0.340 | 2.151 | 1.265 | 2.769 | 1.815 |

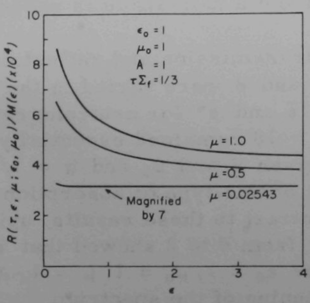


Fig. 2

Normalized Reflection Function as a Function of Exit Energy. ANL Neg. No. 103-A9048.

TABLE VI. $\psi(\tau, \epsilon, \mu)$ and $\varphi(\tau, \epsilon, \mu)$ as Functions of $\mu$; $\tau\Sigma_f = 1/3$ and $\beta = 0.0$

| | $\epsilon = 1$ | | $\epsilon = 2$ | |
|---|---|---|---|---|
| $\mu$ | $\psi(\tau, \epsilon, \mu)$ | $\varphi(\tau, \epsilon, \mu)$ | $\psi(\tau, \epsilon, \mu)$ | $\varphi(\tau, \epsilon, \mu)$ |
| 1.0 | 0.0034262 | 0.0025543 | 0.0029232 | 0.0022789 |
| 0.9 | 0.0034092 | 0.0024609 | 0.0029110 | 0.0022076 |
| 0.8 | 0.0033898 | 0.0023494 | 0.0028961 | 0.0021220 |
| 0.7 | 0.0033651 | 0.0022142 | 0.0028775 | 0.0020173 |
| 0.6 | 0.0033337 | 0.0020472 | 0.0028536 | 0.0018864 |
| 0.5 | 0.0032923 | 0.0018368 | 0.0028220 | 0.0017189 |
| 0.4 | 0.0032358 | 0.0015656 | 0.0027782 | 0.0014982 |
| 0.3 | 0.0031540 | 0.0012100 | 0.0027137 | 0.0011984 |
| 0.2 | 0.0030267 | 0.0007498 | 0.0026100 | 0.0007859 |
| 0.1 | 0.0028115 | 0.0002526 | 0.0024234 | 0.0002819 |

In Tables III-V, values of $\bar{\epsilon}_t$ and $\epsilon_t^*$ for $\mu = 0.02546$ occasionally exceed those for a Maxwellian distribution. This is especially the case for $A = 1$ and $\mu_0 = 0.02546$ in Table V. Because the energy of the incident neutrons is $\epsilon_0 = 1$ in every case, it is physically expected that the values of $\bar{\epsilon}_t$ and $\epsilon_t^*$ should never exceed 2 and 1, respectively. Thus it must be admitted that certain numerical inaccuracies do exist in the procedure used, and these numerical difficulties are magnified for very low values of $\mu$, $\mu_0$, A, and $\tau$. Numerical difficulties for small values of $\mu$ were also encountered by Mayers[29] in one-speed theory, because errors increased sharply when the nonhomogeneous term of Eq. 11 became small.

Tables III and V also show variance calculations for the mean number of scatterings in reflection and transmission. The variance increases rapidly with the number of collisions, a result also noted by Abu-Shumays[19] in one-speed calculations. The large variances are a consequence of the medium being nonabsorbing; in fact, Abu-Shumays[19] has shown for one-speed theory that, in the limit of vanishing absorption, the variance of the mean number of collisions for neutrons reflected from a half-space is unbounded.

The behavior of the neutron transmission and reflection was also investigated when the parameters $\alpha$ and $\beta$ were varied in the absorption law $\Sigma_a(\epsilon) = \beta\epsilon^{-\alpha}$. It was found that $\bar{\epsilon}$ and $\epsilon^*$ for neutrons reflected and transmitted through the slab with $A = 18$ remained essentially constant over a range $0.022 \le \beta \le 0.38$ for a given $\mu$ and $\mu_0$ and $\alpha = 1/2$; this indicates the negligible spectral effect of this type of absorption in a finite medium of a heavy scatterer. In contrast to these results, using a constant value of $\beta = 0.022$ and increasing $\alpha$ from 0 to 2 showed that $\bar{\epsilon}$ diminished monotonically from 1.996 to 1.992 for $\epsilon_0 = 1$, $\mu_0 = 1$, $\mu = 1$, $A = 18$, and $\tau\Sigma_f = 1/3$, thus indicating slight softening of the spectrum.

The behavior of the average number of collisions when absorption is present is just opposite to that of the average energies; the values of $\bar{n}_r$ and $\bar{n}_t$ are quite insensitive to the type of absorption used for a range $0 \le \alpha \le 2$, but change considerably with $\beta$. Figure 3 shows the dependence upon $\beta$ of the average number of collisions suffered by a neutron traversing a slab of width $\tau\Sigma_f = 1/3$ and $A = 18$. The average number of collisions suffered by neutrons before emerging decreases with increasing absorption, as might be expected from physical reasoning.

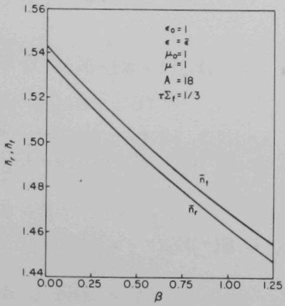


Fig. 3

Average Number of Collisions Suffered by Reflected and Transmitted Neutrons for Absorption Law $\Sigma_a(\varepsilon) = \beta/\sqrt{\varepsilon}$. ANL Neg. No. 103-A9049.

## IV. SUMMARY

A method for the calculation of energy- and angle-dependent emergent distributions from thin slabs has been developed. The method is applicable to slabs of any thickness, although a considerable increase in computer time is required for slab thicknesses of more than a few mean free paths.

An attempt was made to extend the theoretical development to an N-term degenerate kernel, such as that considered by Shapiro and Corngold,[31] but the analysis failed due to problems associated with the noncommutability of the matrices involved. Thus, use of the analysis to treat transport problems involving a realistic, nonseparable kernel is presently constrained by the assumptions necessary to express the kernel in separable form.

# APPENDIX A

## Proof of Lemma 2

Define $C(\ell)$ as that class of functions which are continuous on $0 \le x \le \tau$, $0(\ln x^{-1})$ as $x \to 0+$, and $0[\ln(\tau - x)^{-1}]$ as $x \to \tau-$. Then directly from Theorem 32.1 of Ref. 9, we quote the following:

Lemma A.1. For $\varphi(x) \in C(\ell)$, and $H(t) \equiv \int_0^t \varphi(u)\,du$, and $0 \le x \le \tau$,

$$\int_0^x L_t\{\varphi(u)\}\,dt = L_x\{H(t)\} - L_0\{H(t)\} + [K_2(\tau - x) - K_2(\tau)]\,H(x), \qquad (A.1)$$

where $L_t$ and $K_2$ are defined in Eqs. 12 and 13, respectively. We shall use Lemma A.1 to help establish Lemma 2 (Sec. II). We define $G_n(t)$ as the Neumann solution of

$$(I - L)_x\{G_n(t)\} = B'(x) + S(0)K_1(x) - S(\tau)K_1(\tau - x), \qquad (A.2)$$

where we have suppressed explicit reference to all $\epsilon$ and $\mu$ dependence in the functions, where

$$(I - L)_x\{S(t)\} = B(x), \qquad (A.3)$$

and where $B(x) \in C(\ell)$. If we define

$$F(x) = \int_0^x G_n(t)\,dt - S(x) + S(0) \qquad (A.4)$$

and subsequently show that $F(x) = 0$, we have $S'(x) = G_n(x)$; then Lemma 2 is a direct consequence of Eq. A.2 if we identify $S(x) = J(x, \epsilon, \mu)$ and $B(x) = \exp[-\Sigma_t(\epsilon)x/\mu]$. Therefore, we shall prove that $F(x) = 0$.

To prove that $F(x) = 0$, we first note that for the identity operator we have the relation

$$\int_0^x I_t\{\varphi(u)\}\,dt = \int_0^x \varphi(t)\,dt = I_x\left\{\int_0^t \varphi(u)\,du\right\}.$$

Now we integrate Eq. A.2 over x and, with subsequent application of Eq. A.1 and all possible explicit integration carried out, we get

$$(I - L)_x\left\{\int_0^t G_n(u)\,du\right\} = B(x) - B(0) + S(0)[K_2(0) - K_2(x)] - S(\tau)[K_2(\tau - x) - K_2(\tau)]$$

$$- L_0\left\{\int_0^t G_n(u)\,du\right\} + [K_2(\tau - x) - K_2(\tau)]\int_0^x G_n(u)\,du. \qquad (A.5)$$

We next note from Eq. A.3 that

$$(I - L)_x\{S(t)\} = B(x) - B(0) + S(0) - L_0\{S(t)\}. \tag{A.6}$$

Also, from Eq. 12,

$$L_x\{S(0)\} = S(0)L_x\{1\} = S(0)[2K_2(0) - K_2(x) - K_2(\tau - x)],$$

which reduces to the special case

$$L_0\{S(0)\} = S(0)[K_2(0) - K_2(\tau)].$$

The last two results, when combined, give

$$(I - L)_x\{S(0)\} = S(0)[1 - K_2(0) + K_2(x) + K_2(\tau - x) - K_2(\tau)] - L_0\{S(0)\}. \tag{A.7}$$

The application of the Operator $(I - L)_x$ to Eq. A.4 and subsequent use of the Eqs. A.5-A.7 produce

$$(I - L)_x\{F(t)\} = [K_2(\tau - x) - K_2(\tau)]\, F(\tau) - L_0\{F(t)\} = AK_2(\tau - x) - B, \tag{A.8}$$

where $A \equiv F(\tau)$ and $B \equiv K_2(\tau)F(\tau) - L_0\{F(t)\}$.

Now, using the nomenclature of Ref. 9, we note that the method of successive substitutions applied to Eq. A.3 yields a Neumann series which we shall denote by

$$S(x) = \sum_{\nu=0}^{\infty} L_x^{\nu}\{B(t)\},$$

which, if it converges to a solution of Eq. A.3, is called the Neumann solution. Necessary and sufficient conditions for the existence of the Neumann solution of Eq. A.3 have not been shown; however, Busbridge[9] shows that if $K_2(0) \le 1/2$ and $B(x)$ is continuous and of order 1 as $x \to 0+$ and of order 1 as $x \to \tau-$, then the Neumann solution of Eq. A.3 exists. Hence, noting the linearity of the operator $L_x$, we write the Neumann solution of Eq. A.8 as

$$F(x) = A \sum_{\nu=0}^{\infty} L_x^{\nu}\{K_2(\tau - x)\} - B \sum_{\nu=0}^{\infty} L_x^{\nu}\{1\} = AF_1(x) - BF_2(x). \tag{A.9}$$

Equation A.9 will be used to show that $A = B = 0$; hence, $F(x) = 0$.

From Eq. A.4, $F(0) = 0$; and thus

$$AF_1(0) - BF_2(0) = 0. \tag{A.10}$$

Evaluating Eq. A.9 for $x = \tau$ and using the definition $A = F(\tau)$ give

$$A[1 - F_1(\tau)] + BF_2(\tau) = 0. \tag{A.11}$$

From Eq. A.9 we note that $F_2(x) = F_2(\tau - x)$, which implies that $F_2(0) = F_2(\tau)$. A solution of Eqs. A.10 and A.11 is thus given by

$$A[1 - F_1(\tau)+F_1(0)] = 0. \tag{A.12}$$

It is shown in Ref. 9 that $1 - F_1(x) + F_1(0) \neq 0$ if $K_2(0) \leq 1/2$. Thus Eq. A.12 demands that $A = 0$; then Eq. A.10 demands that $B = 0$. Since both $A = 0$ and $B = 0$, it follows from Eq. A.9 that $F(x) = 0$, and the lemma is proved.

## APPENDIX B

### A Symmetry Proof

To derive Eqs. 17 and 18, we define the inner product

$$(U, V) = \int_0^{\tau} U(t)V(t)\,dt.$$

Then, because of the symmetry of the kernel of Eq. 12,

$$(U, L_{\tau}\{V\}) = (V, L_{\tau}\{U\}).$$

Now write Eq. 11 as

$$J_i(\tau) = L_{\tau}\{J_i(t)\} + B_i(\tau),$$

where $B_i(\tau) = \exp[-\Sigma_t(\epsilon_i)\tau/\mu_i]$ and $i = 1, 2$ denotes different values of the variables $\epsilon$ and $\mu$. We can then write

$$(J_1, J_2) = \left(J_1, L_t\{J_2(t')\}\right) + (J_1, B_2)$$

and

$$(J_2, J_1) = \left(J_2, L_t\{J_1(t')\}\right) + (J_2, B_1).$$

Now, if the integral exists, we have $(J_1, J_2) = (J_2, J_1)$ and

$$\left(J_1, L_t\{J_2(t')\}\right) = \left(L_t\{J_1(t')\}, J_2\right) = \left(J_2, L_t\{J_1(t')\}\right),$$

so it follows that

$$(J_1, B_2) = (J_2, B_1). \tag{B.1}$$

Equation 17 follows directly from Eq. B.1. If we let $J_1 = J(\tau - t)$ and $B_1 = \exp[-\Sigma_t(\epsilon)(\tau - t)/\mu]$ in Eq. B.1, we obtain Eq. 18 after a change of variables.

To prove Eq. 19, one first evaluates Eq. 11 at $x = 0$ and then uses Eq. 13, interchanges the order of integration, and finally uses Eq. 17 to show that

$$J(0, \epsilon, \mu) = 1 + \frac{1}{2\overline{\overline{\Sigma}}} \int_0^{\infty} d\epsilon_0 \int_0^1 \frac{d\mu_0}{\mu_0} M(\epsilon_0)\Sigma_s^2(\epsilon_0)\zeta\left[\frac{\Sigma_t(\epsilon_0)}{\mu_0}, \epsilon, \mu\right]. \tag{B.2}$$

Evaluating Eq. 11 at $x = \tau$ and applying the above procedure while using Eq. 18, it may also be shown that

$$J(\tau, \epsilon, \mu) = \exp[-\Sigma_t(\epsilon)\tau/\mu]\left\{1 + \frac{1}{2\overline{\Sigma}}\int_0^\infty d\epsilon_0 \int_0^1 \frac{d\mu_0}{\mu_0} M(\epsilon_0)\Sigma_s^2(\epsilon_0)\zeta\left[-\frac{\Sigma_t(\epsilon_0)}{\mu_0}, \epsilon, \mu\right]\right\} \tag{B.3}$$

Equation 19 follows directly from a comparison of Eqs. B.2 and B.3.

## REFERENCES


1. F. R. Mynatt, *The Discrete Ordinates Method Problems Involving Deep Penetrations*, ORNL-RSIC-19 (1968).

2. H. Kahn, *Applications of Monte Carlo*, RM-1237-AEC (1954).

3. A. M. Weinberg and E. P. Wigner, *The Physical Theory of Neutron Chain Reactors*, Univ. of Chicago Press (1958).

4. G. M. Wing, *An Introduction to Transport Theory*, John Wiley and Sons, New York, N.Y. (1962).

5. S. Chandrasekhar, *Radiative Transfer*, Clarendon Press, Oxford (1950).

6. D. R. Mathews, K. F. Hansen, and E. A. Mason, *Deep Penetration of Radiation by the Method of Invariant Imbedding*, Nucl. Sci. Eng. *27*, 263 (1967).

7. A. Mockel, *Invariant Imbedding and Polyenergetic Neutron Transport Theory - Part I: Theory*, Nucl. Sci. Eng. *29*, 43 (1967), and ibid. 51 (1967).

8. R. Aronson, *One-Velocity Neutron Transport Problems by the Transfer Matrix Method*, Nucl. Sci. Eng. *27*, 271 (1967).

9. I. W. Busbridge, *The Mathematics of Radiative Transfer*, Cambridge Univ. Press, London (1960).

10. M. M. R. Williams, *The Energy Dependent Milne Problem with a Simple Scattering Kernel*, Nucl. Sci. Eng. *18*, 260 (1964).

11. J. Arkuszewski, *Milne Problem for Thermal Neutrons with Application*, Nucl. Sci. Eng. *27*, 104 (1967).

12. M. M. R. Williams, *The Slowing Down and Thermalization of Neutrons*, John Wiley and Sons, New York, N.Y. (1966).

13. J. Mika, *The Thermalization Theory with a Simple Scattering Kernel*, Nucl. Sci. Eng. *22*, 235 (1965).

14. Y. Sobouti, *Scattering and Transmission Functions for Non-Coherent Scattering*, Astrophys. J. *153*, 257 (1968).

15. V. V. Sobolev, *The Number of Scatterings During Photon Diffusion, I*, Astrophysics *2*, 69 (1966).

16. V. V. Sobolev, *The Number of Scatterings During Photon Diffusion, II*, Astrophysics *2*, 119 (1966).

17. V. V. Sobolev, *The Number of Scatterings During Photon Diffusion, III*, Astrophysics *3*, 5 (1967).

18. V. V. Sobolev, *The Number of Scatterings During Photon Diffusion, IV,* Astrophysics *3,* 69 (1967).

19. I. K. Abu-Shumays, *Generating Functions and Reflection and Transmission Functions,* J. Math. Anal. Appl. *18,* 453 (1967).

20. S. Pahor, *Multiple Scattering and the Inverse Albedo Problem,* Phys. Rev. *175,* 218 (1968).

21. I. Kuŝĉer,"Transport Problems for Thermal Neutrons," *Developments in Transport Theory,* ed. by E. Inonu and P. F. Zweifel, Acad. Press, New York, N.Y. (1967).

22. B. Davison, *Neutron Transport Theory,* Oxford Univ. Press, London (1957).

23. E. Fermi, *On the Motion of Neutrons in Hydrogeneous Substances,* Ricarca Sci. *VIII-2,* 13 (1936).

24. N. Corngold, P. Mickael, and W. Wollman, *The Time Decay Constants in Neutron Thermalization,* Nucl. Sci. Eng. *15,* 13 (1963).

25. S. Pahor, *Albedo and Milne's Problem for Thermal Neutrons,* Nucl. Sci. Eng. *31,* 110 (1968).

26. T. W. Mullikin, *Radiative Transfer in Finite Homogeneous Atmospheres with Anisotropic Scattering: II. The Uniqueness Problem for Chandrasekhar's $\psi_\ell$ and $\phi_\ell$ Equations,* Astrophys. J. *139,* 1267 (1964).

27. S. Pahor and I. Kuŝĉer, *On the Non-Uniqueness of the Solution of Chandrasekhar's S-Equation in Radiative Transfer,* Astrophys. J. *143,* 888 (1967).

28. R. W. Milkey, *On the Uniqueness of Solutions in Radiative Transfer,* Astrophys. J. *148,* 935 (1967).

29. D. F. Mayers, *Calculation of Chandrasekhar's X- and Y-Functions for Isotropic Scattering,* Mon. Notic. Roy. Acad. Sci. *123,* 471 (1962).

30. R. E. Bellman, R. E. Kalaba, and M. C. Prestrud, *Invariant Imbedding and Radiative Transfer in Slabs of Finite Thickness,* American Elsevier Publ. Co., New York, N.Y. (1963).

31. C. Shapiro and N. Corngold, *Approach to Equilibrium of a Neutron Gas,* Phys. Rev. *137,* A1686 (1965).